ACS APPLIED MATERIALS & INTERFACES

Biological and Medical Applications of Materials and Interfaces

Photoactivable Polymers Embedded with Cadmium-free Quantum Dots and Crystal Violet: Efficient Bactericidal Activity against Clinical Strains of Antibiotic-Resistant Bacteria

Ethel Owusu, Alexander J. MacRobert, Elaine Allan, Ivan P. Parkin, Elnaz Yaghini, and Imad Naasani

ACS Appl. Mater. Interfaces, **Just Accepted Manuscript** • DOI: 10.1021/acsami.9b02109 • Publication Date (Web): 11 Mar 2019

ACS Publications

is published by the American Chemical Society. 1155 Sixteenth Street N.W., Washington, DC 20036

Photoactivable Polymers Embedded with Cadmium-free Quantum Dots and Crystal Violet: Efficient Bactericidal Activity against Clinical Strains of Antibiotic-Resistant Bacteria

Ethel G. A. Owusu,[†,‡,§] Alexander J. MacRobert,[†*] Imad Naasani,[#] Ivan P. Parkin,[‡] Elaine Allan,[§] Elnaz Yaghini[†*]

† UCL Division of Surgery and Interventional Science, University College London, Charles Bell House, 43-45 Foley Street, London W1W 7TS, United Kingdom

‡ Materials Chemistry Research Centre, Department of Chemistry, University College London, 20 Gordon Street, London WC1H 0AJ, United Kingdom

§ Department of Microbial Diseases, UCL Eastman Dental Institute, University College London, 256 Gray's Inn Road, London WC1X 8LD, United Kingdom

Nanoco Technologies Ltd, 46 Grafton Street, Manchester M13 9NT, United Kingdom

*E-mail: a.macrobert@ucl.ac.uk; elnaz.yaghini@ucl.ac.uk

Abstract

The rising incidence of antibiotic-resistant infections from contaminated surfaces in hospitals or implanted medical devices has led to increasing interest in new antibacterial surfaces. Photoactivatable surfaces that can generate cytotoxic reactive oxygen species under exposure to ambient light is a promising approach to inactivation of surface-borne microorganisms. There is growing interest in the use of quantum dots (QDs) as light-harvesting agents for photobactericidal applications but the cadmium in commonly used QDs will restrict clinical application. Herein, the photobactericidal activity of novel polyurethane substrates containing cadmium-free quantum dots was tested against clinical multi-drug resistant Gram-positive and Gram-negative bacterial strains: methicillin-resistant *Staphylococcus aureus* (MRSA) and a carbapenemase-producing strain of *Escherichia coli* (E. coli). To enhance the capacity for reactive oxygen species generation, QDs were incorporated into the polymer with a photosensitising dye, crystal violet. Close proximity between the QD and dye enables electron and energy transfer processes leading to generation of cytotoxic singlet oxygen and superoxide radicals. A QD solution in cyclohexane was premixed with a solution of CV in the more polar solvent, dichloromethane, to promote the formation of QD-CV nanocomposite complexes via CV adsorption. This solution was then used to embed the quantum dots and crystal violet into medical grade polyurethane via swell-encapsulation. The combination of QD and CV elicited significant synergistic antibacterial activity under visible light against MRSA within 1 h (99.98% reduction) and E. coli within 4 h (99.96% reduction). Photoluminescence lifetime and singlet oxygen phosphorescence measurements demonstrated interaction between the quantum dots and the crystal violet occurs within the polymer that can lead to enhanced generation of reactive oxygen species. Strong inhibition of kill was observed using the superoxide scavenger, superoxide dismutase. The efficacy of these QD-CV polymer substrates that can harvest light across the visible spectrum, against multi-drug resistant bacteria demonstrates the feasibility of this approach.

Key words: antibacterial, surfaces, polymer, light-activated, photodynamic therapy, quantum dots, crystal violet, reactive oxygen species

Introduction

Each year, over 4 million patients in the European Union and 2 million in the United States acquire a healthcare-associated infection (HAI), contributing to roughly 110,000 and 99,000 associated deaths respectively.[1-2] Healthcare-associated infections which are also referred to as nosocomial infections lead to prolonged suffering for patients and in many cases longer hospital stays. The rising incidence of antimicrobial resistance (AMR) whereby bacteria become resistant to previously effective medications further exacerbates the impact of HAIs: more than 70% of the bacteria that causes HAIs are resistant to at least one commonly prescribed antibiotic.[3] Excessive and often unnecessary antibiotic use increases the selective pressure on bacterial populations, creating a pool of resistant genes some of which can transfer horizontally between populations and create multi-drug resistant (MDR) HAIs that are increasingly difficult to treat, lead to significant patient morbidity and substantial costs for healthcare systems.[4]

Among the most common sources of infectious agents causing HAIs are inanimate surfaces and objects (for example, patient room touch surfaces, medical equipment and devices) that have become contaminated.[5] One strategy to reduce the nosocomial reservoir of bacteria is the use of self-disinfecting antimicrobial surfaces. The use of photosensitisers (PS) of low toxicity such as toluidine blue O (TBO), methylene blue (MB) and crystal violet (CV) in photodynamic therapy (PDT) has been shown to be effective against a wide range of microbes.[6-9] Endowment of polymers, which are widely used in medical devices, with antibacterial activity has been achieved by encapsulation with photosensitisers and irradiation with visible non-ionising light.[10-14] Bactericidal activity is mediated by reactive oxygen species (ROS) generated *via* photodynamic processes: illumination with light at the appropriate wavelength activates the photosensitiser to an excited singlet state which subsequently converts to a long-lived triplet state which leads to generation of ROS *via* photoelectron transfer (PET) (Type I) or energy transfer (Type II) pathways. In Type I, photo-induced redox result in the generation of free radicals such as superoxide and hydroxyl radicals. The Type II pathways involve direct energy transfer from the triplet state to molecular oxygen generating highly reactive singlet oxygen ($^1O_2$).[15] ROS such as superoxide, hydroxyl radicals and singlet oxygen can oxidise biological substrates thereby inducing irreversible cellular membrane damage and enzyme deactivation, ultimately causing cell death. Nevertheless, despite their efficacy, the utility of PS as antimicrobial agents can be limited by their narrow absorption bands and susceptibility to photobleaching. Quantum dots (QDs) are emerging as a new class of versatile photoluminescent probes for many biomedical applications such as drug delivery, sensors, cancer therapy and imaging.[16-19] Compared to organic dyes including conventional photosensitisers, QDs have intense and broad light absorption, high photobleaching threshold and photoluminescence (PL) quantum yield and long photoluminescence lifetimes.[20] Additionally, by tailoring QDs shape, size and composition, QDs can be engineered to emit at wavelengths that can span the entire spectrum.[21]

These unique photophysical properties and their broad-band light harvesting capability have prompted interest in the use of quantum dots as photosensitising agents.[22] Under high power visible light doses, QDs have been effective in inhibiting the growth of a range of Gram-positive and Gram-negative bacteria through the generation of ROS.[23-26] As with conventional photosensitising organic dyes, QDs may generate ROS *via* Type I and Type II pathways and there are several reports of direct formation of superoxide radical anions by photoelectron transfer (PET) from photoactivated cadmium and indium-based QDs.[23-24, 27] Dismutation of superoxide can generate hydrogen peroxide which in turn can generate highly reactive hydroxyl radicals *via* the iron-catalysed Fenton process. With the exception of some graphene dots reported in the literature,[28-29] QDs exhibit very low quantum yields of $^1O_2$ (regarded as the most potent ROS), compared to clinically used photosensitisers.[27, 30] Conjugation of QDs with photosensitising dyes has been shown to significantly increase singlet oxygen efficiencies. In this configuration, excited QDs can act as energy donors and excite PS acceptors to their

excited singlet state by transferring energy *via* the mechanism known as Förster Resonance Energy Transfer (FRET).[22, 31-32]

A major drawback with their biomedical use is that QDs generally contain restricted heavy metals such as cadmium which severely hinders the clinical translation of such QDs owing to the possible release of toxic Cd^{2+} ions which can also induce oxidative stress *via* generation of ROS.[33-34] Recently, we and others have reported on the use of indium-based cadmium-free QDs and demonstrated their safety in rodent models, which should facilitate their translation to clinical use.[35-36] Herein, we report the development of novel photoactivatable antimicrobial surfaces based on polyurethane embedded with a combination of crystal violet (CV) and new cadmium-free indium-based QDs (CFQD® nanoparticles). Polyurethane was selected since it is widely used for medical device applications. We hypothesised that the addition of QDs to CV encapsulated in polymer would boost antimicrobial activity by increasing production of cytotoxic reactive oxygen species. The QD-CV complexes were produced by adapting the simple non-covalent incorporation technique, namely 'swell-encapsulation-shrink'.[13] The antibacterial activity of QD-CV embedded polyurethane substrates was tested against representative multidrug resistant nosocomial Gram-positive and Gram-negative pathogens.

Methods and Materials

Materials

CFQD® nanoparticles dispersed in cyclohexane were synthesised and provided by Nanoco Technologies Ltd (Manchester, UK). Medical grade polyurethane sheets (thickness 0.8 mm) were purchased from American Polyfilm Inc. (Branford, USA). Crystal violet dye and solvents were purchased from Sigma-Aldrich (UK).

Synthesis of CFQD® nanoparticles

Indium-based QDs (CFQD® nanoparticles) dispersed in cyclohexane with peak photoluminescence at 620 nm were synthesised and provided by Nanoco Technologies Ltd. using proprietary synthesis procedures based on the molecular seeding process.[37] Briefly, a ZnS molecular cluster $[Et_3NH_4][Zn_{10}S_4(SPh)_{l6}]$ was heated in the presence of indium myristate ($In(MA)_3$) and Tris(trimethylsilyl)phosphine ($(TMS)_3P$) in a medium of di-n-butylsebacate ester. The indium-based alloyed cores were washed with hydrofluoric acid and then heated in a solution of zinc acetate and Bis(trimethylsilylmethyl) sulfide ($(TMS)_2S$) in butylsebacate ester to form a coating layer of ZnS.[35] Finally, the nanoparticles were isolated by precipitation in acetone and then re-dispersed in cyclohexane. The resulting nanoparticles had surface capping ligands of mainly myristate and butyl sebacate, which will confer an electronegative polarity, and were isolated by precipitation in acetone and then re-dispersed in cyclohexane. The quantum efficiencies of the final unfunctionalised indium-based nanoparticle material ranged from 73% to 79% in cyclohexane. The molecular weight of the CFQD® nanoparticles is ~500 kDa, therefore a 1 mg/mL concentration is approximately equivalent to 2 μM.

Incorporation of nanoparticles and dye into polymer

The CFQD® nanoparticles and the CV were incorporated non-covalently into polyurethane *via* a simple dipping process known as 'swell-encapsulation-shrink'.[13] Stock QDs solutions were prepared in cyclohexane (Cy) with a concentration of 2 mg/mL and CV stock solutions were prepared in dicholoromethane (DCM) with a concentration of 1 mM. Dipping solutions were prepared to have final concentrations of either 1 mg/mL QD + 0.5 mM CV; 1 mg/mL QD; or 0.5 mM CV in a solvent system of 1:1 cyclohexane: dichloromethane, to produce polymer samples with QDs and CV (QD + CV PU), QDs only (QD PU) and CV only (CV PU). In all cases, a 1 cm^2 polymer squares were placed into the appropriate solutions and left to swell in the dark for 24 h inside a closed bottle containing 10 mL of dipping solution. Subsequently, samples were left to dry in the dark at room temperature for 24 h, washed with dH_2O and air dried. As controls, polymer samples were swollen in pure 1:1 Cy:DCM solvent.

Material Characterisation

Transmission electron microscopy (TEM) of quantum dots

A solution of the quantum dots in cyclohexane was drop cast onto 300 mesh carbon coated copper grid (Agar Scientific) and air-dried prior to imaging. High resolution transmission electron microscope (TEM) images were acquired using a JEOL 2100 TEM with a LaB6 source operating at an acceleration voltage of 200 kV. Micrographs were taken on a Gatan Orius charge-coupled device (CCD) camera with Digital Micrograph software. Particle size analysis was carried out Gatan Suite software.

Spectroscopic measurements

UV−vis absorption spectra of suspensions and polymer substrates were recorded using dual beam spectrophotomers (PerkinElmer Lambda 950 or Shimadzu UV-2600). Emission spectra of suspensions were recorded with a spectrofluorimeter (Horiba FMax4 Fluorimeter). Quartz cuvettes were employed of 1 cm path length. For the emission spectroscopy measurements of the polyurethane substrates, which are strongly light-scattering, samples were mounted diagonally at 45° incidence to the excitation beam, and a long-pass Schott filter (RG435) was installed in the emission port to filter out the blue excitation scattered light. The overlap integral $J(\lambda)$ for the FRET study was calculated using open source software (FluorTools.com).

Singlet Oxygen Phosphorescence Measurements

The singlet oxygen phosphorescence at 1270 nm of modified medical grade polyurethane incorporated with QD and/or CV was detected using time-resolved photon counting. For detection in the near-IR, a thermoelectrically cooled photomultiplier (model H10330-45, Hamamatsu Photonics Ltd, Hertfordshire, UK) was used, and the emission was collected *via* a series of lenses from the cuvette in combination with a long-pass (950 nm cut-on, Andover Corp., USA) and a band-pass filter centred at 1270 nm (Interferenzoptik Electronik GmbH, Germany). Polyurethane samples were mounted diagonally in a quartz cuvette and irradiated using a 532 nm Nd:YAG laser (Lumanova GmbH, Germany) with the beam axis aligned at 45º to the surface plane of the sample in order to optimise detection of $^1O_2$ within the polymer. The laser was pulsed at a repetition rate of 3 kHz and a pulse length of 3 ns and a fast photodiode (1 ns rise time, Becker-Hickl, Germany) was used to synchronise the laser pulse with the photon counting detection system. Neutral density filters was used to attenuate the laser power to 2 mW. The photon counting equipment consisted of a PC-mounted multiscaler board (model MSA-300, Becker-Hickl, Germany) and a pre-amplifier (Becker-Hickl, Germany) which gave a resolution of 5 ns per channel. Time-resolved phosphorescence measurements were accumulated by the multiscaler board at a 0.1 μs bin width and the signals were analysed using FluoFit software (PicoQuant GmbH, Germany) to extract the lifetime parameters.

Time-Resolved Lifetime Measurements

Photoluminescence lifetime of QDs was measured using time-correlated single photon counting (TCSPC). Solutions of QDs and QD-CV complexes at various CV concentrations (fixed QD concentration) were prepared and placed in a 1 cm optical path quartz cuvette. A pulsed laser diode module Edinburgh instrument Ltd., UK model EPL-405 was used to excite the samples at 405 nm at a 1 MHz repetition rate (EPL- 405, Edinburgh Instruments Ltd., UK). The emission was detected using a fast multialkali photomultiplier module (model H5773–04, Hamamatusu Photonics K.K., Japan) *via* a long-pass filter (OG510, Schott, UK) and a monochromator (model M300, Bentham Instrument Ltd, UK). A Lyot depolarizer (Thorlabs Ltd, Ely, UK) was incorporated to minimise any polarisation anisotropy artefacts. TCSPC was carried out using a PC-mounted TCSPC board (TimeHarp 260, PicoQuant GmbH, Germany) and lifetimes were derived using Fluofit software (PicoQuant GmbH, Germany). The Instrument Response Function (IRF) was obtained from a non-fluorescent scattering Ludox solution (Sigma-Aldrich, UK). Optimum fitting with minimisation of the residuals was confirmed using a Chi-squared value $\chi^2 < 1.4$. The photoluminescence lifetime of QDs was also measured after embedding of QDs and/or CV in the polymer. The substrates were mounted

on microscope glass slides and signals were detected as described for QD and QD-CV solutions above.

Bacterial Strains

Methicillin-resistant *Staphylococcus aureus* (MRSA NCTC 13143) was obtained from the National Collection of Type Cultures (PHE, Colindale); a clinical strain of epidemic methicillin-resistant *Staphylococcus aureus* (EMRSA 4742) was obtained from P. Wilson, University College London Hospital; and the multi-drug resistant (MDR) carbapenemase-producing clinical strain of *Escherichia coli* (*E. coli* 1030) was obtained from J. Wade, King's College Hospital, London). These organisms were stored at −70 °C in Brain−Heart Infusion broth (BHI, Oxoid) containing 20 % (v/v) glycerol and propagated onto either MacConkey agar (MAC, Oxoid) in the case of *E. coli* or mannitol salt agar (MSA, Oxoid) in the case of MRSA, for a maximum of 2 subcultures at intervals of 2 weeks.

Antibacterial Activity

The following 1 cm^2 polyurethane (PU) squares were used in the microbiology experiments:

i. solvent treated polyurethane (control PU)
ii. crystal violet encapsulated polyurethane (CV PU)
iii. Quantum dot encapsulated polyurethane (QD PU)
iv. Quantum dot and crystal violet encapsulated polyurethane (QD + CV PU)

For testing of each strain, Brain−Heart Infusion broth (BHI, Oxoid) was inoculated with 1 bacterial colony and cultured in air at 37 °C for 18 h with shaking, at 200 rpm. The bacterial pellet was recovered by centrifugation, (20 °C, 2867.2g, 5 min), washed in phosphate buffered saline (PBS) (10 mL), and centrifuged again to recover the pellet (20 °C, 2867.2g, 5 min), and the bacteria were finally re-suspended in PBS (10 mL). The washed suspension was diluted 1000-fold to obtain an inoculum of $\sim 10^6$ cfu/mL. In each experiment, the inoculum was confirmed by plating 10-fold serial dilutions on agar for viable counts. Triplicates of each polymer sample type were inoculated with the inoculum (25 µL) and covered with a sterile coverslip (2.2 cm^2). The samples were then incubated in the light and dark for up to 4 h. Under light conditions, a white fluorescent light source (General Electric, USA)[25], emitting at an average light intensity of 6000 ± 990 lux measured at 25 cm from the samples, was employed. After incubation, the inoculated samples and coverslips were added to PBS (450 µL) and mixed using a vortex mixer. The neat suspension and 10-fold serial dilutions were plated on agar for viable counts and incubated aerobically at 37 °C for 24 h (*E. coli*) or 48 h (MRSA).

Detection of Superoxide

To investigate the mechanism of bactericidal activity against bacteria, superoxide dismutase (SOD) in PBS (50 U/mL) was added to the bacterial suspension and exposed to the polyurethane substrates using the protocol described above to deactivate any superoxide radicals emanating from the polymer surface. SOD from bovine erythrocytes was purchased from Sigma-Aldrich, UK and filter sterilised using a 0.2 µm PES syringe filter (VWR, UK).

Statistical Analysis

Each experiment contained a minimum of two technical replicates and the experiments were carried out three times. The statistical significance, in both light and dark conditions, was analysed using independent sample t-test of the following comparisons:

a. Control vs. inoculum
b. Crystal violet alone vs. control
c. Quantum dot alone vs. control
d. Quantum dot with crystal violet combination vs. crystal violet alone
e. Quantum dot with crystal violet combination vs. control

Results were considered significantly different for $P < 0.05$. Error bars show the standard deviation from the mean.

Results & Discussion

Characterisation

TEM images of the CFQD® nanoparticles in solution showed the particles to be spherical and mono-disperse (Fig. 1A). Analysis of over 150 particles gave an average size of 3.6 nm with a narrow size distribution SD of ± 0.6 nm (Fig. 1B).

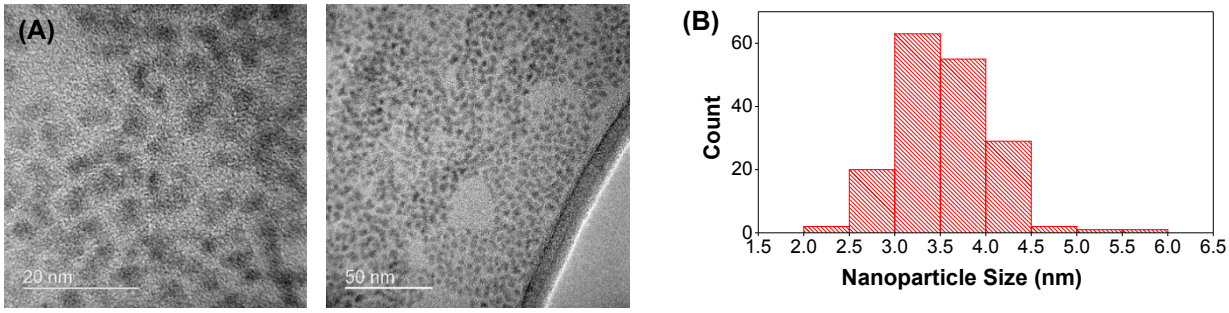

Figure 1. **(A)** High resolution TEM image of CFQD® nanoparticles. **(B)** Size distribution of CFQD® nanoparticles from TEM

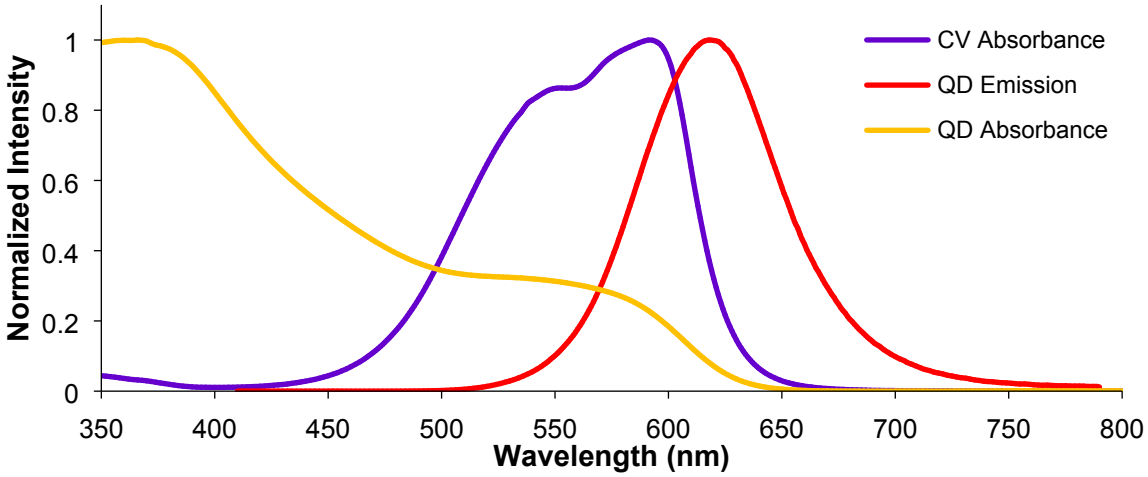

Figure 2. Normalized absorbance (yellow line) and emission spectra (red line) of CFQD® nanoparticles and absorbance spectrum of crystal violet (purple line) in 1:1 cyclohexane/dichloromethane solvent. The emission spectrum of CV is not shown as it exhibits negligible fluorescence in low viscosity solutions.

The QD emission spectrum is characterised by a symmetric profile with a full-width at half maximum of about 60 nm and a sharply defined maximum emission of 620 nm. The absorption spectrum of the QD showed broad peaks in the visible region up to about 600 nm and strong absorption in the blue region (Fig. 2). CV is a highly coloured triphenylamine dye with an extensive history as an anti-bacterial and anti-fungal agent, which we have used in previous antimicrobial polymer studies in combination with gold and zinc oxide nanoparticles.[14, 38] CV is also inexpensive, chemically stable[39] and has been widely used as a therapeutic agent in the clinic for conditions such as oral candiadis (thrush), eczema and as a blood additive to prevent transmission of Chagas' disease.[10, 39-41] The absorption spectrum of crystal violet is narrow compare to the QD spectrum and has an overlapped doublet spectrum with the

maximum absorption peak at 590 nm and a shoulder around 550 nm (Fig. 2).[42] CV dimerisation in solution leads to small blue shifts in the spectrum.[43] The emission spectrum of CV was not recorded in solution since most arylmethane dyes have typically low emission due to the strong dependence of fluorescence quantum yields on solvent viscosity. In low viscosity fluid solvents, the arylmethane groups can rotate freely resulting in the formation of twisted intramolecular charge transfer (TICT) states with negligible fluorescence quantum yields due to rapid radiationless decay to the ground state. However, this molecular rotor effect is diminished when CV is dissolved in high viscosity solvents or bound to proteins and CV fluorescence from the first excited singlet state can then be measured [44-46] Likewise, when CV is encapsulated in polymer where the spatial constraint imposed by the matrix will restrict the rotor effect, the CV fluorescence is evident.[14, 46]

Incorporation of Nanoparticle and Dye into Polymer

The swell-encapsulation-shrink technique[12-13] that we have previously employed as a two-step process was modified to a one-step process in order to improve co-localisation of the QD and CV in the polymer and complex formation. This was achieved by mixing the QDs and CV in a miscible 1:1 cyclohexane/dichloromethane solvent system as illustrated in Figure 3A. A mixed solvent system was required since the QDs are soluble in cyclohexane whereas CV was not directly soluble. The CV was therefore first dissolved in DCM and subsequently this solution was mixed with the cyclohexane QD solution. The polymer samples were then treated with this solution for 24 h resulting in purple-stained samples which after drying were used for antimicrobial testing. QD photoluminescence and CV fluorescence measurements of the polymers after modification confirmed uptake of the QD and/or CV (Fig. 3B, 3C).

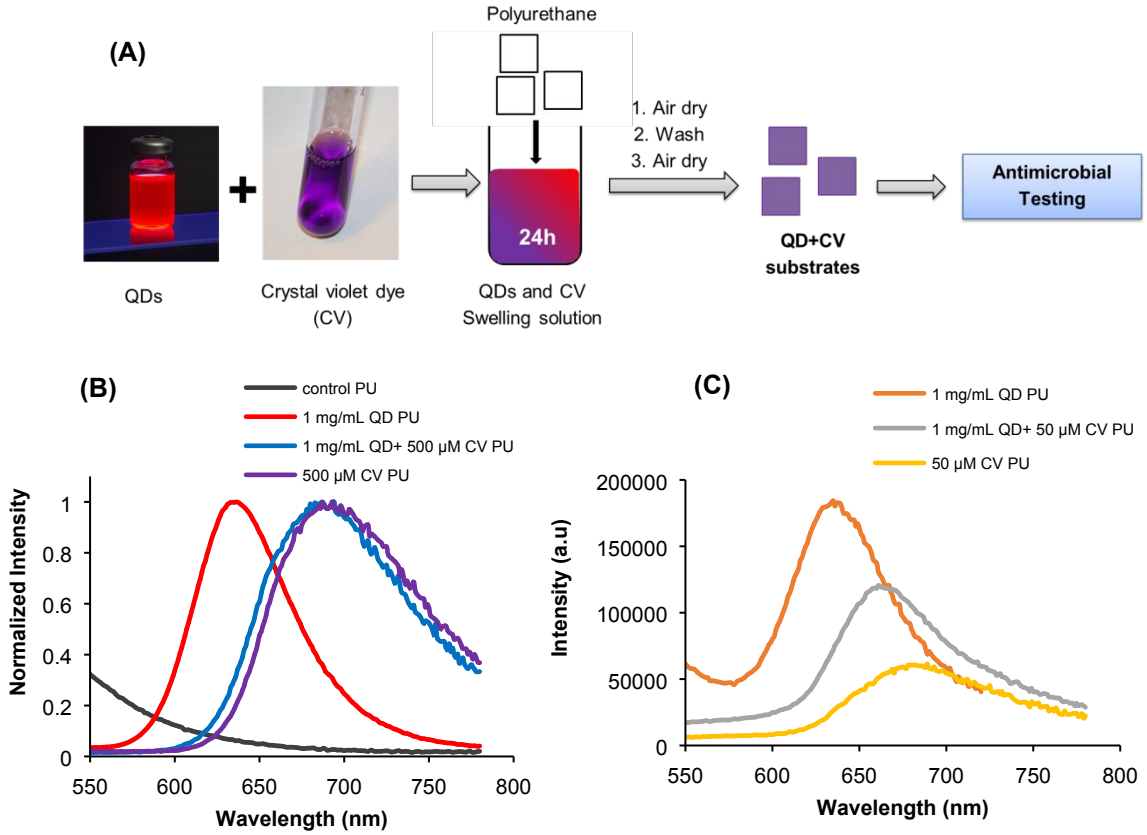

Figure 3. **(A)** Scheme shows the preparation of QD nanoparticle and crystal violet encapsulated polyurethane samples. Squares indicate the polyurethane squares used. **(B)** Normalized emission spectra of polyurethane substrates confirming uptake of QD and/or CV. Emission of the control polyurethane (grey line), polyurethane encapsulated with 1 mg/mL QDs (red line), 500 µM CV (purple line) and a combination of 1 mg/mL QDs and 500 µM CV (blue line) measured at excitation wavelength of 400 nm. **(C)** Emission spectra of polyurethane samples doped with a lower CV concentration

following excitation at 400 nm: 1 mg/mL QDs (orange line), 50 μM CV (yellow line) and a combination of 1 mg/mL QDs and 50 μM CV (grey line).

In the CV-doped polymer, the CV emission spectrum appears to be markedly red-shifted to ~700 nm at higher concentrations (Fig. 3B) compared to that observed for polymer samples doped at lower concentrations as shown in Figure S1: for 5 μM CV PU, the peak is at ~ 645 nm which is very similar to that observed when CV at 10 μM is bound to serum albumin in aqueous solution.[46] This red-shift effect is concentration-dependent and is ascribed to absorption of the shorter wavelength portion of the CV emission spectrum which suppresses emission nearer 600 nm and leads to the apparent red-shift. When both QD and CV (50 μM) are present, the red-shift appears to be lower with peak emission at 667 nm compared to 686 nm for CV alone (Fig. 3C).

Antibacterial Testing

The antibacterial activity of QD and CV encapsulated polyurethane samples (QD + CV PU) was tested against methicillin-resistant isolate of *Staphylococcus aureus,* strain MRSA NCTC 13143 and a multi-drug resistant (MDR), carbapenemase-producing clinical strain of *Escherichia coli* (E. coli 1030). These bacterial strains were selected as representative multi-drug resistant (MDR) nosocomial Gram-positive and Gram-negative pathogens, respectively.[47] The antibacterial activity of solvent-treated polyurethane (control PU), CV encapsulated polyurethane (CV PU) and QD encapsulated polyurethane (QD PU) was also tested and compared to QD + CV PU substrates.

Figure 4A shows the bactericidal activity of the various polymers against MRSA NCTC 13143 in the dark and following 1 h of exposure to a white light source with an average light intensity of 6600 ± 990 lux. Following 1 h of incubation in the dark, neither the control PU nor the QD PU samples showed significant kill of MRSA, whereas the CV and QD + CV PU samples showed a 1.2 $\log_{10}$ and 0.7 $\log_{10}$ reduction in bacterial numbers, respectively. Limited CV dark toxicity has been previously observed in our previous study on a laboratory strain of *S. aureus* which also used polyurethane substrates.[38] Exposure to white light for a period of 1 h also did not result in any bactericidal activity from the control PU or QD PU but the addition of CV alone (CV PU) produced a 2.7 $\log_{10}$ reduction in bacterial numbers. Furthermore, the combination of quantum dot and CV (QD + CV PU) caused the greatest kill of MRSA with numbers reduced by 3.7 $\log_{10}$ (99.98%; P = 0.027 compared to CV PU), following exposure to white light for just 1 h.

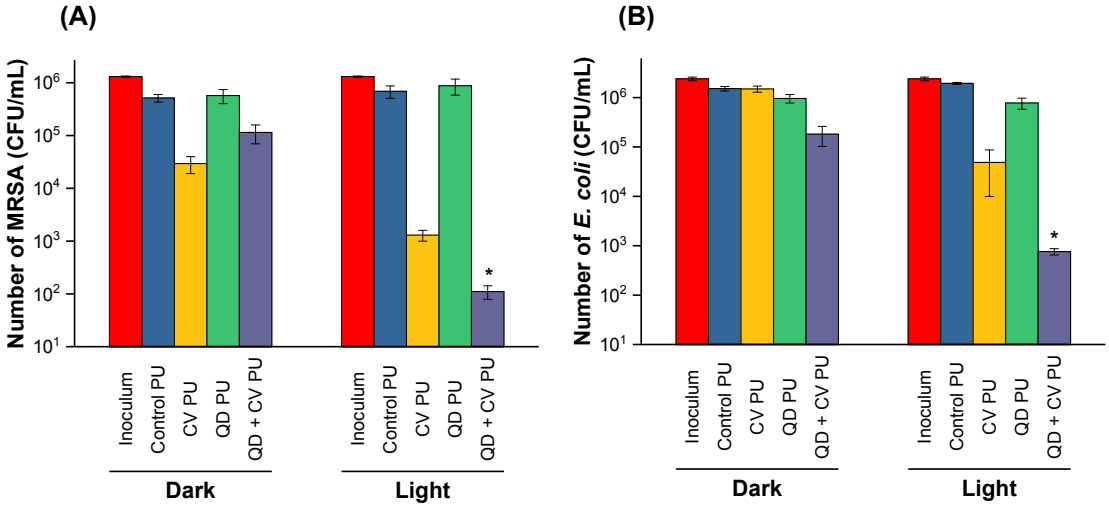

Figure 4. **(A)** Viable counts of MRSA NCTC 13143 on unmodified and modified polyurethane substrates incubated at 20°C under dark conditions and under white light (6000 lux ± 990 lux) for 1 h; **(B)** Viable counts of E. coli 1030 on unmodified and modified polyurethane substrates incubated at 20°C under

dark conditions and under white light (6000 lux ± 990 lux) for 4 h. Concentrations of swelling solutions (made in 1:1 Cy/DCM solvent) used to modify PU: QDs – 1 mg/mL; CV – 500 μM. (* indicates significance is $p < 0.05$ compared to CV PU)

The photo-bactericidal activity of the polyurethane substrates was tested against MDR *E. coli* 1030, under the same conditions but for an extended period. As a Gram-negative bacterium, *E. coli* has a double membrane, consisting of both a cytoplasmic membrane and an outer membrane containing lipopolysaccharide which presumably accounts for the longer exposure time required for bactericidal activity. This contrasts with MRSA NCTC 13143, a Gram-positive bacterium, which possesses only a single cell membrane, allowing effective kill in a shorter period of time.[48] Figure 4B shows the activity of the samples after 4 h of incubation in the dark. Only the QD + CV PU substrate showed activity in the dark, inducing a 0.9 $\log_{10}$ reduction in *E. coli* numbers after 4 h in the dark. White light illumination for a period of 4 h resulted in no significant bactericidal activity on the control PU material as expected, a 1.6 $\log_{10}$ reduction in bacterial numbers was observed with CV PU, and a 0.4 $\log_{10}$ reduction with QD PU. QD + CV PU showed increased bactericidal activity compared to CV PU alone, resulting in a 3.4 $\log_{10}$ reduction in bacterial numbers following light exposure for 4 h ($P = 0.019$ compared to CV PU). Comparison of the fractional viabilities (i.e. the surviving fractions) shows that the combination of QDs with CV was synergistic for all strains tested (Table S1).

The potential of QDs in suspension to act as potent bactericidal light-activated agents has been studied previously. For instance, Ristic and co-workers reported the treatment of a clinical isolate of MRSA and reference strain *E. coli* ATCC 25922 with electrochemically produced graphene QDs in phosphate buffered saline (PBS). Following exposure of bacteria to 200 mg/mL of graphene QDs and irradiation with blue light (465 – 475 nm) for 15 min, *E. coli* numbers were reduced by 80% and *S. aureus* numbers by about 95%.[26] Similarly, Courtney *et al*. prepared green-emitting cadmium telluride (CdTe) QDs directly prepared in aqueous media to which populations of MDR bacteria were exposed with and without visible light. In the presence of 100 nM CdTe and light for 8 h, the growth of patient isolates of MRSA and *Klebsiella pneumoniae* were reduced by 29% and 59% respectively. Under the same conditions, a clinical isolate of MDR *Salmonella typhimurium* showed 56% growth inhibition and two MDR *E. coli* isolates had 83% and 64% growth inhibition, respectively.[23] They demonstrated that superoxide was generated by photoexcitation of the QDs, and attributed the bactericidal activity to oxidative damage by this species and other ROS generated *via* the Fenton process.

However, in our study, polymer samples with QD alone were ineffective using the light doses (6000 lux) employed which we assume is due in part to limited uptake into the polymer *via* the simple swell-encapsulation technique,[49] coupled with the use of visible light illumination where QD absorption is weaker compared to UV illumination (Figure 2, yellow line). A further key limiting factor in the use of QD-only doped polymer is that cumulative singlet oxygen and, more critically, superoxide generation by polymer-bound QDs is likely to be low in contrast to studies where QDs interact directly with cells. Yaghini *et al.* have shown that superoxide generation efficiency is significantly higher when QDs can interact with the important biomolecule nicotinamide adenine dinucleotide (NADH) which is present at high concentrations in cells *via* a Type 1 process.[30]

The significant enhancement in bactericidal activity in the presence of CV shows that the addition of a photosensitising dye is essential for lethal photosensitisation in polymers, since QDs on their own elicit little to no antibacterial effect in polyurethane at these light doses. The use of CV only did elicit bacterial kill, as we have observed in other studies,[14, 38] but significantly less than the combination of the QD and CV. The observed enhancement of the intrinsic antibacterial properties of CV by the introduction of QDs suggests the occurrence of additional sources of ROS generation *via* interaction between the QD and CV *via* Förster resonance

energy transfer (FRET) and/or photoelectron transfer (PET) involving the transfer of an electron or hole in this system.

Photophysical studies

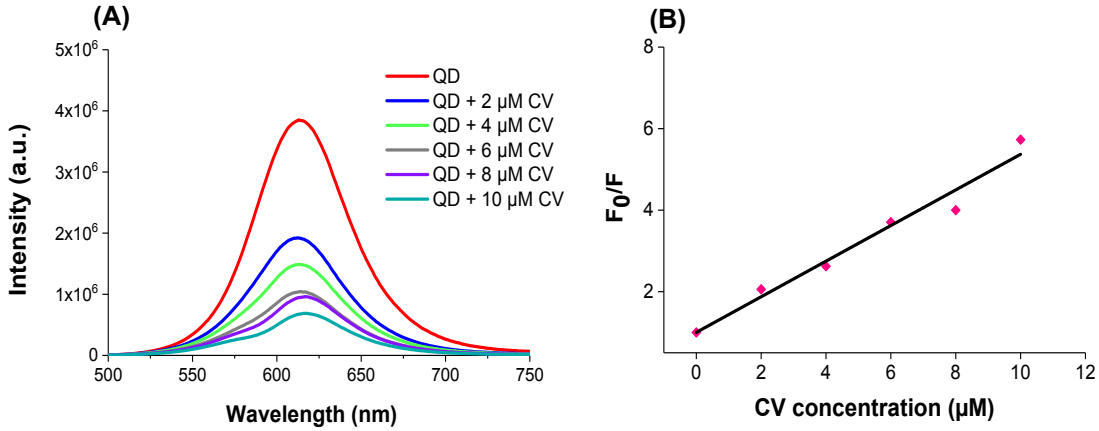

Figure 5. **(A)** Steady-state photoluminescence spectra of pure QDs and QD-CV combinations with increasing CV concentration in 1:1 Cy/DCM solvent system. Spectra from each sample was recorded following excitation at 400 nm where CV has negligible absorbance. Concentration of QDs stayed constant at 0.02 mg/mL as CV concentration was increased. **(B)** Stern-Volmer plot (at 620nm, λ_{ex} = 400 nm) showing the relative changes in the emission intensity of the QDs as a function of CV dye concentration.

As a cationic dye in an aprotic solvent system, CV will be electrostatically attracted to the polar surface of QDs, which is capped with electronegative ligands, to form electrostatically bound complexes, which will enable the occurrence of short-range energy transfer interactions to take place.[50-51] In order to ascertain whether a QD-CV complex can function as a donor-acceptor hybrid for FRET, the spectral overlap of CV with the QD must be demonstrated. As shown in figure 2, there is spectral overlap between the emission spectrum of the QDs and absorption spectrum of CV which, in principle, should enable the occurrence of FRET between donor QDs and the acceptor dye when blue light excitation employed. The overlap integral *J(λ)*, a quantitative measure of the degree of spectral overlap between the donor emission and the acceptor absorption was calculated using the equation:

$$J(\lambda) = \int_0^\infty f_D(\lambda)\varepsilon_A(\lambda)\lambda^4 d\lambda \qquad (1)$$

where $f_D(\lambda)$ is the dimensionless fluorescence intensity of the donor in the absence of the acceptor, $\varepsilon_A(\lambda)$ the extinction coefficient of the acceptor, in units of $M^{-1}cm^{-1}$ and λ is the wavelength in nanometres.[52] $J(\lambda)$ of the QD-CV complex was calculated to be 1.35 x 10^{14} $nm^4M^{-1}cm^{-1}$, a relatively high overlap integral in accordance with the good spectral overlap of the QD-CV pair, which would favour non-radiative energy transfer from photoexcited QD donor to ground state photosensitiser acceptor.[53]

The corresponding Förster distance (R_0), the distance at which the FRET efficiency is 50%, was then derived as 3.4 nm, using the equation:

$$R_0 = 0.0211\left(\kappa^2 \phi n^{-4} J(\lambda)\right)^{1/6} \qquad (2)$$

where κ is the orientation faction (κ^2 = 2/3), Φ is the quantum dot fluorescence quantum yield, n the refractive index and *J(λ)* the spectral overlap.[52]

Steady-state and time-resolved QD photoluminescence studies were carried out to investigate the nature of the interaction between QDs and CV and the mechanism of the photoactivity of QD and CV mixtures in solution and the polymer. A fixed concentration of QDs and increasing concentrations of CV were prepared in solution and excited at 400 nm, where the QD is excited but CV has negligible absorbance. Results in solution show a significant decrease in QD emission but no apparent CV fluorescence at longer wavelengths (Figure 5). CV absorption of the QD emission at 620 nm and longer wavelengths cannot account for the large decrease in intensity over this range of CV concentrations.[43] It has been previously reported that the FRET efficiency increases when the number of acceptors per QD increases. We also observed that the decrease in QDs emission intensity was dependent on the CV/QD ratio and with increasing CV/QDs ratio, the QDs emission decreased progressively. If FRET occurs, then an increase in the acceptor emission should be observed. The apparent absence of the CV emission may however simply be due to the low fluorescence efficiency of the CV even when bound to the QD which has a very high quantum yield in comparison.[46] Alternatively, photoinduced electron transfer (PET) between QDs and CV may take place, as found for a CdSe/Zn QD/fluorescein electrostatically bound complex in heptane,[51] resulting in generation of the semi-reduced CV radical with different spectral properties, as discussed later in detail.

The static or dynamic nature of the quenching processes was measured using Stern-Volmer plots. The decrease in photoluminescence/fluorescence intensity is described by the Stern–Volmer (SV) relationship in equation (3)

$$F_0/F = 1 + K_{SV}[Q] \quad (3)$$

$$K_{SV}[Q] = k_q \times \tau_0 \quad (4)$$

where F_0 and F are the fluorescence intensities in the absence and presence of acceptor respectively, $[Q]$ the quencher concentration and K_{SV} the Stern–Volmer quenching constant.

Dynamic quenching involves deactivation of the QD exciton upon contact with the quencher, in this case the CV molecules present in solution. Conversely, in static quenching, a complex is formed between the QD and the quencher, which in this case would arise from adsorption of the CV onto the QD surface, and the photoluminescence quenching can arise from either energy or electron transfer processes.[52 54] The SV plot (F_0/F against [Q]) at 620 nm (λ_{ex} = 400 nm) for QDs donor with CV acceptor in a solvent system of 1:1 cyclohexane/dichloromethane is shown in Fig. 5B. The linear SV relationship with a slope, K_{SV} of 4.4 x 10^5 M^{-1} is indicative of a single class of fluorophores, all equally accessible to the quencher. This was confirmed by estimating the bimolecular quenching constant (k_q) from equation (4) using the slope obtained from the Stern–Volmer analysis ($K_{SV}[Q]$) and the amplitude weighted lifetime of the donor QD (τ_0) in solution, as set out in equation 5, which was measured to be 46 ns using time-correlated single photon counting. The large value of quenching constant (k_q) of 8.91 x 10^{12} M^{-1} s^{-1} observed on addition of CV, is two orders of magnitude higher than the diffusion controlled limit for bimolecular reactions, and shows that the interaction was predominantly static in nature with CV bound to the QD surface.[55]

From these studies, we conclude that direct interaction between the QDs and CV takes place in solution *via* adsorption of CV onto the QD surface which will enable occurrence of FRET and/or PET. In the strongly light-scattering polymer samples, quantitative absorption spectroscopy studies are difficult unless the samples are very thin unlike the samples here. The spectra shown in Figure 3C indicate that QD photoluminescence quenching in the presence of CV does take place in the polymer samples but to confirm occurrence of quenching FRET or PET, time-resolved fluorescence data was acquired by QDs donor lifetime

measurements. Analysis of time-resolved fluorescence data can discriminate against apparent donor emission intensity attenuation due to facile reabsorption effects. For example, in a previous study in aqueous solutions, we observed that the mixtures of PEGylated CdSe/ZnS QDs with toluidine blue O could enhance bacterial kill following visible illumination. However, QD time-resolved emission measurements found no evidence for FRET interaction and the associated lifetime shortening, and the enhanced activity was attributed to reabsorption of QD emission by the dye.[25]

In this study, excitation of the QDs was carried out at 405 nm where QD absorption is strong whereas CV absorption is very weak. The QD lifetime is also long compared to CV fluorescence lifetime which is < 5 ns in viscous solvents or when bound to protein.[46, 56]

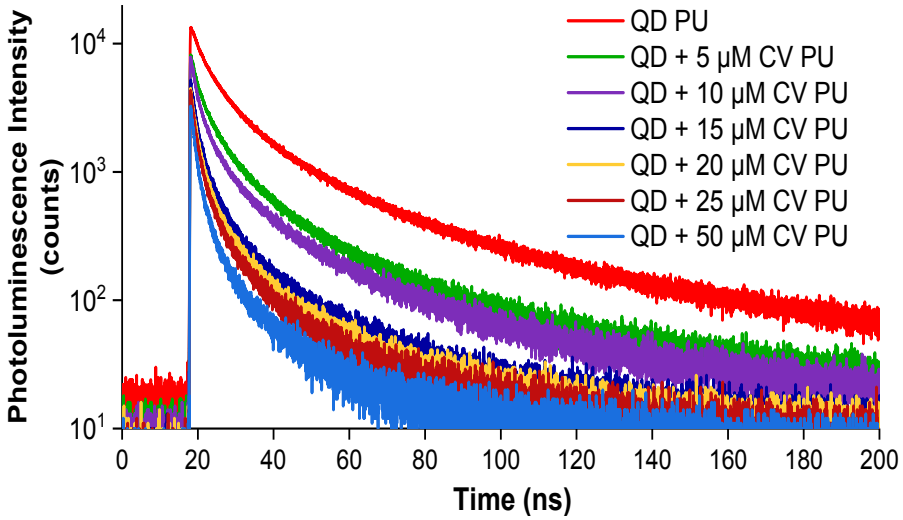

Figure 6. Logarithmic plots of time-resolved photoluminescence measurements of pure QDs and QD-CV combination embedded in polyurethane *via* swell-encapsulation-shrink. Time-resolved QD emission lifetimes at 620 nm were measured after swelling polyurethane in solutions with final concentrations of 0.02 mg/mL QDs (blue line), 0.02 mg/mL QDs and 5 μM CV (red line), 0.02 mg/mL QDs and 10 μM CV (green line), 0.02 mg/mL QDs and 15 μM CV (purple line), 0.02 mg/mL QDs and 20 μM CV (light blue), 0.02 mg/mL QDs and 25 μM CV (orange line), 0.02 mg/mL and 50 μM CV (grey line).

Measurements were taken of the QD photoluminescence decay when only QDs were embedded in polyurethane as well as the QD decay when QDs with varying concentrations of CV were incorporated into polyurethane. Subsequently, the donor exciton lifetime was derived by fitting the time-resolved photoluminescence intensity (I_t) of the QD to a bi-exponential decay of the form,

$$I_t = A_1 e^{(-t/\tau_1)} + A_2 e^{(-t/\tau_2)} \qquad (5)$$

where A and τ are the fractional amplitude and emission lifetime respectively.[57]

It was observed that the QD emission lifetime in the presence of CV (τ_{DA}) was significantly shorter than the QD emission lifetime in the absence of CV (τ_{DA}). The exciton photoluminescence lifetime progressively shortened with the introduction of increasingly higher concentrations of the dye into the polymer (Fig. 6). In the absence of the photosensitiser, the mean fractional amplitude weighted lifetime of QDs was found to be τ_D = 32.0 ns which was significantly reduced to τ_{DA} = 6.8 ns in the presence of 50 μM CV.

If the quenching is due to FRET, the FRET efficiency (E) of donor/acceptor complexes in polymer can be derived from the time-resolved fluorescence measurements, using the equation:

$$E = 1 - \frac{\tau_{DA}}{\tau_D} \quad (6)$$

where τ_{DA} and τ_D are the average fluorescence lifetime (amplitude weighted) of the donor in the presence and absence of the acceptor, respectively in polyurethane.[57-58]

Table 1 displays the FRET efficiencies of the QD-CV with increasing CV concentration. At the highest crystal violet concentration, the FRET efficiency was calculated as 79%. Note however that the CV concentration given is that of the dipping solution and we assume an approximately linear dependence between these values and the polymer uptake. We also assume that the use of the single-stage swell-encapsulation loading with both agents combined resulted in uptake of intact QD-CV complexes and CV residing in the matrix but in close proximity to the QDs.

It is important to note that the lifetime quenching observed is also consistent with the occurrence of PET therefore on the basis of these studies alone, we cannot be certain that FRET does take place in addition to PET.[54] However since the PET mechanism should not lead to singlet oxygen generation, any $^1O_2$ produced by the QD-CV polymers would give distinct evidence of FRET. Therefore, in addition to steady-state and time-resolved fluorescence studies, the generation of singlet oxygen by the polymer samples was examined.

Table 1 Mean fractional amplitude weighted QD emission lifetimes and calculated FRET efficiencies of pure QD and QD-CV complexes with increasing CV concentrations (in the swell-encapsulation medium) when incorporated into polyurethane *via* the swell-encapsulation-shrink method

CV Concentration (μM)	**Mean τ (ns)**	**FRET Efficiency (%)**
0	32.0	0
5	28.2	12
10	21.6	33
15	17.0	47
20	14.7	54
25	7.8	75
50	6.8	79

Singlet Oxygen Phosphorescence Studies

The generation of $^1O_2$ in the polymer was investigated using time-resolved near-IR detection based on the singlet oxygen phosphorescence at 1270 nm. We have previously shown that CV alone in silicone can generate singlet oxygen using excitation at 532 nm.[59] However, in aqueous solution, the efficiency of $^1O_2$ is very low owing to deactivation of the CV excited singlet state by the molecular rotor effect. In viscous solvents or the polymeric microenvironment, this effect is inhibited which permits $^1O_2$ generation.

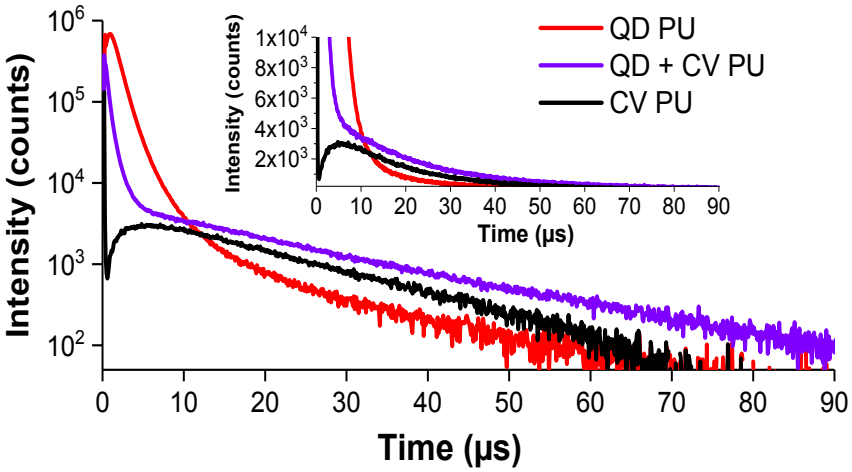

Figure 7 Logarithmic time-resolved phosphorescence singlet oxygen recorded at 1270 nm following pulsed laser irradiation of modified polyurethane containing CV only (black line), QD only (red line and a combination of QD and CV (purple line). (Concentrations: QDs – 1 mg/mL; CV – 50µM CV). The traces have been subtracted from the control (untreated polyurethane). **Inset:** Linear scale plot over the same time range

Figure 7 shows traces recorded for samples containing CV alone, QD and CV with QD using similar concentrations that are used for the antimicrobial assays. Logarithmic intensity plots are shown since this allows the differences in quasi-monoexponential decay lifetimes to be more readily discerned. For the QD alone trace, a relatively short-lived high intensity signal is observed, lasting ~10 µs. This signal is ascribed to the near-IR tail of the QD photoluminescence.[60] Although this signal will be very weak, the singlet oxygen phosphorescence is also very weak given the very low quantum yield. Direct generation of singlet oxygen by photoexcitation of indium-based QDs is energetically unfavourable although direct generation of superoxide may be possible, as discussed later.[27] We have previously shown for CdS-based QDs that no direct singlet oxygen generation could be observed with an upper limit to the quantum yield estimated as <0.003.[30] Using spin-trap electron paramagnetic resonance (EPR) spectroscopy and reporter assays, Chibli *et. al*. found no evidence for the generation of singlet oxygen in indium phosphide based QDs.[27] For CV alone, a characteristic initial increase followed by a near-exponential decay is observed, in agreement with our previous study[59] using CV and other dyes such as methylene blue (MB).[61] The initial rise in signal is governed by the rate of quenching of the CV triplet state to the ground state by oxygen to generate singlet oxygen in the polymer matrix. The subsequent decay in signal is governed by the rate of quenching of the singlet oxygen phosphorescence by the polymer matrix. The lifetime of singlet oxygen in the polyurethane where only CV was present, derived by fitting the signal to a mono-exponential decay, was determined to be 36 µs. This value is similar to that observed for CV embedded in silicone polymer (~ 40 µs).[59] The decay kinetics were not affected by the CV concentration within the ranges used. There is also a very short spike in signal at t = 0 which is due to CV fluorescence. The presence of the QD with CV resulted in a major change in the initial time-dependence with the rise-time seen for CV alone replaced by an intense short-lived decay lasting ~3 µs followed by a decay with a lifetime that closely matches that observed for CV alone which is consistent with the assumption that the same decay kinetics for singlet oxygen should apply for each type of polymer sample. However, the key observation from this comparative study is that the overall intensity of the singlet oxygen signal with the QD/CV combination was higher than for CV alone.

The short but rapid decay in signal seen at early times < 10 μs in the presence of CV matches that observed in our previous QD FRET studies[60] and is consistent with the QD donor photoluminescence being quenched by the CV. As can be seen from the logarithmic decay dependence, the quenched QD photoluminescence lifetime in the decay profile of QD + CV PU is considerably shorter than that for in the absence of CV (QD PU). Use of a lower concentration of CV of 5 μM (not shown) resulted in a slower decay of the QD photoluminescence, which is consistent with the quenching mechanism. We can therefore conclude that singlet oxygen is generated in the polymer both by CV alone and by the interaction of QD and CV. In the aforementioned solution phase studies, the driving force for QD/CV complex formation would be electrostatic attraction of the cationic CV to the polar QD surface. In the polymer matrix however, a proportion of the CV may also reside in the matrix in close proximity to the QDs but not bound at the QD surface. Since the Förster distance is estimated at 3.4 nm, FRET would be viable for CV that is physically separated from the QD. A degree of spatial separation of the CV from the QDs in the polymer may also enable greater partitioning of the interaction mechanism to FRET over PET which would be favoured by the shorter range interaction when CV is surface-adsorbed. CV located further away from the QD beyond the energy transfer range could reabsorb the QD emission in a non-FRET process, in an analogous mechanism proposed by Narband *et al.* In their study of CdSe/ZnS QDs mixed with toluidine blue O in aqueous solution, bactericidal activity was ascribed to facile absorption of QD emission by the photosensitiser.[25] In the present study however, the QD emission is so strongly quenched by FRET or electron transfer (discussed below in more detail) that a reabsorption mechanism can be precluded. A further point to take into consideration is that the diffusion pathlength of the singlet oxygen in the polymer will be short (< 1 micron)[59] thus the active zone for ROS generation at the surface is shallow. This therefore severely limits the pathlength over which such reabsorption processes can take place.

Superoxide Generation & Inhibition Assay

In addition to resonant energy transfer, it is also possible that a PET process can take place between the QD and CV when in close proximity. Photoexcited indium phosphide QDs are capable of reducing oxygen to superoxide[27] and the reduction potential of the $O_2/O_2^{-\bullet}$ redox couple is – 0.18 V vs. NHE (normal hydrogen electrode) in aqueous solution (equation 7) which is close to that of $CV^+/CV^\bullet$ reduction potential at – 0.36 V (equation (8)).[62-63] CV is a good electron acceptor and photoreduction of CV by the QDs to generate the semi-reduced CV radical is likely to occur given the similar potentials. By extrapolation of excited-state redox potentials estimated for other indium-based QDs emitting at comparable wavelengths to the QDs used here, reduction of CV should be energetically feasible: the valence band reduction potential for InP quantum dots is estimated as 0.95 V [27, 64]. This assumes that effects of binding and the different solvent on redox potentials are minimal.

The CV radical generated by PET from the QD can then interact with molecular oxygen to generate superoxide by electron transfer which should be energetically possible due to the positive redox potential (+ 0.18 V) of the reaction (equation (9)).

$$CV^+ + e^- \rightarrow CV^\cdot \qquad -0.36\ \text{V} \qquad (7)$$

$$O_2 + e^- \rightarrow O_2^{-\cdot} \qquad -0.18\ \text{V} \qquad (8)$$

$$CV^\cdot + O_2 \rightarrow CV^+ + O_2^{-\cdot} \qquad +0.18\ \text{V} \qquad (9)$$

Experimental evidence for this Type 1 process in aqueous solution has been obtained by detection of superoxide using electron paramagnetic resonance (EPR) spectroscopy following illumination of solutions of crystal violet containing the electron donor, NADH, which donates an electron to the excited CV triplet state to form the CV radical.[65-66] In the study by Fischer

et al., micellar solutions of Triton-X were employed.[66] We have to assume that this reaction scheme is also possible in the polymer matrix. However, the occurrence of Type 1 processes following illumination when CV is incubated directly with bacteria (where the CV is presumably bound with substrates and can interact with electron donors) lends support to the scheme we propose, whereby superoxide is generated *via* interaction of oxygen with the semi-reduced CV radical formed by photoreduction.[46, 67]

We also need to consider the effects of direct photoexcitation of CV to its singlet state in the QD/CV complex. Since CV emission occurs at longer wavelengths than the QD absorption there is little spectral overlap to enable FRET to take place with the CV acting as the donor to the QD. FRET would also have to compete with the rapid internal non-radiative pathways of excited singlet CV state. Alternatively, electron transfer may be possible since spectral overlap is not required, and in this case the QD may act as an electron donor to the CV in its excited singlet or triplet state to form the CV radical thereby leading to superoxide formation in an analogous mechanism to aforementioned reaction where NADH acts as an electron donor to photoexcited CV. The CV triplet state is likely to act as the acceptor since it is longer lived than the excited singlet state. Since CV absorbs within the QD absorption band it would not be possible to excite CV alone therefore this process would be more difficult to discern experimentally. Instead of the QDs the polymer matrix, which will contain unreacted monomer, may also be able to promote a Type 1 process, and contribute to the cytotoxicity observed with CV alone. Photoexcitation of dimers of CV may also act as a source of superoxide *via* electron-transfer reactions as postulated previously for MB-doped polymer substrates.[61] Direct generation of superoxide by electron transfer to oxygen by the CV triplet state has been postulated by Reszka *et al.* and Fischer *et al.* [65-66] but was confirmed by Brezova and colleagues who demonstrated photogeneration of superoxide directly from CV in aprotic solvents using EPR.[68] Therefore superoxide should be generated in illuminated polymer samples with CV alone and CV with QDs, and then be able to diffuse into the surrounding solution containing the bacteria. This mechanism is distinct from treating bacteria incubated in solutions containing a photosensitiser where the sensitiser can interact directly with the bacteria and exert photooxidative damage after internalisation or via electron or hydrogen abstraction reactions mediated by the sensitiser triplet state in contact with the membrane.[69] The latter mechanism is unlikely to be effective for bactericidal polymer systems unless the polymer is designed specifically to release the sensitiser.

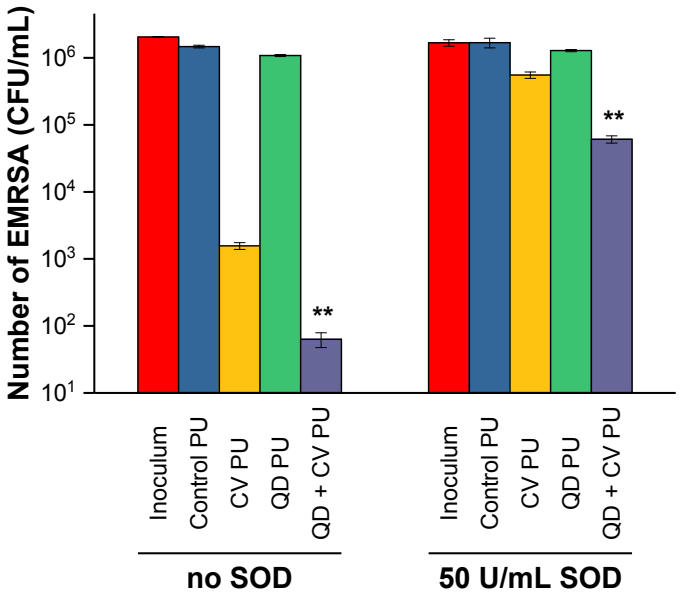

Figure 8 Viable counts of EMRSA 4742 on unmodified and modified polyurethane polymers tested under standard conditions (20°C, 1 h white light treatment at 6000 lux) without SOD (left) and in the presence of 50 U/mL SOD (same temperature and lighting conditions as standard test) (right).

Concentrations of swelling solutions (made in 1:1 Cy/DCM solvent) used to modify PU: QDs – 1 mg/mL; CV – 500 μM. (** indicates significance of $p < 0.01$ compared to CV PU)

To assess the possible contribution of Type I electron transfer pathways, the bactericidal activity of the control PU, CV PU and QD + CV PU substrates were tested against EMRSA 4742 after 1 h of white light treatment, both under standard conditions as well as in the presence of superoxide dismutase (SOD). SOD acts as a scavenger of superoxide, a radical generated by PET as discussed above. After 1 h exposure to light, neither the control PU nor QD PU demonstrated any significant bactericidal activity, and there was no change in activity in the presence of 50 U/mL SOD. Conversely, CV PU and QD + CV PU bactericidal activities were significantly diminished in the presence of SOD. The antibacterial activity of CV PU and QD + CV PU substrates decreased by ~2.5 $\log_{10}$ (from 99% to 66.9%) and ~3 $\log_{10}$ (from 99.996% to 96.4%) respectively when 50 U/mL SOD was added (Fig. 8).

The effectiveness of SOD in inhibiting the potent kill of CV PU and QD + CV PU upon irradiation indicates that $O_2^{-\bullet}$ is formed by the materials then subsequently scavenged before oxidative damage occurs to the bacteria. Although superoxide is relatively unreactive, superoxide can undergo dismutation in solution before reaching the bacteria to hydrogen peroxide, which is an effective bactericidal agent. Furthermore, the iron-catalysed Fenton process will result in generation of the highly reactive hydroxyl radical species. In this case inhibition of superoxide using superoxide dismutase will also inhibit these ROS which is consistent with our data in Figure 8. Thus, conversion of superoxide to more potent ROS can compensate for its lower activity. Since we know that $^1O_2$ is generated as well, we conclude that the synergistic enhancement in antibacterial activity of QDs combined with CV is due to the combined action of ROS generated by both Type I and Type II mechanisms. The range of mechanisms of ROS generation using QDs and CV is distinct to our previous work using 2 nm diameter gold nanoparticles or ZnO nanoparticles and crystal violet in polymer substrates. In those studies where the nanoparticles exhibit negligible absorption in the visible range, FRET interaction would not apply and electron transfer interactions are likely to have taken place only via excitation of the CV.[14, 38]

Conclusion

This study is the first to investigate the antibacterial effects of heavy metal-free quantum dots when embedded in a clinically relevant polymer, in order to assess the practicality and effectiveness of quantum dots in reducing bacterial contamination of surfaces. We have shown that indium-based quantum dot nanoparticles and crystal violet can be embedded into polyurethane *via* the swell-encapsulation-shrink technique using a simple 'one-pot' dipping process. Characterisation of polymer samples showed good uptake of QD and dye without the use of expensive, chemical or mechanical deposition methods. Owing to their larger size, it is likely that the QDs reside near the surface whereas free CV will also be encapsulated deeper within the polymer since it can disperse more readily owing to its smaller size.[49]. Since the ROS have a limited diffusion distance within the polymer before reaching the surface, the localisation of the QDs nanoparticles near the surface should be advantageous for a synergistic effect mediated by ROS.[14] These novel QD-CV polymer substrates demonstrated highly effective antimicrobial activity against clinical strains of both Gram-positive and Gram-negative bacteria. The combination of the QDs and crystal violet caused 99.98% kill of two strains of methicillin-resistant *Staphylococcus aureus* after 1 h and 99.96% kill in a carbapenemase-producing *Escherichia coli* strain in 4 h using broad-band visible illumination at 6000 lux. Steady-state and time-resolved QD fluorescence and singlet oxygen phosphorescence analysis confirmed that the QDs and CV can interact to promote generation of reactive oxygen species. Singlet oxygen Type II reactions enabled enhancement of crystal violet's intrinsic antimicrobial properties when combined with QDs, while antimicrobial tests in the presence of SOD indicated the involvement of Type I reactions for QD + CV PU substrates. The contribution from both processes amplifies QD + CV PU substrate activity, however

further analysis will be required to evaluate which mechanism has a greater contribution to the photo-bactericidal activity of the materials.

The efficacy of these QD-CV polymer substrates that can harvest light across the visible spectrum, against multi-drug resistant bacteria demonstrates the potential of quantum dot-photosensitiser combinations for use in disinfecting hospital surfaces and devices. This therapeutic approach generates ROS that cause bacterial death by attacking multiple sites on the microorganisms, making the development of resistance unlikely. Thus, QD-CV polymers show promise assisting to decrease the risk of infections by reducing the levels of environmental contamination. The technique will also be applicable for other medically used polymers such as silicone.

Supporting Information

Fluorescence emission spectra of crystal violet-incorporated polyurethane and statistical analysis of bactericidal activity of materials

Acknowledgements

We acknowledge support from the Medical Research Council for the award of a CASE studentship (grant award MR/M015866/1) to support this work (EO).

References

1. Organisation for Economic Co-operation and Development (OECD), *Health at a Glance: Europe 2016: State of Health in the EU Cycle*. OECD Publishing: 2016.
2. Klevens, R. M.; Edwards, J. R.; Richards, C. L.; Horan, T. C.; Gaynes, R. P.; Pollock, D. A.; Cardo, D. M., Estimating Health Care-Associated Infections and Deaths in US Hospitals, 2002. *Public Health Rep.* **2007,** *122* (2), 160-166.
3. Samanipour, A.; Dashti-Khavidaki, S.; Abbasi, M. R.; Abdollahi, A., Antibiotic Resistance Patterns of Microorganisms Isolated from Nephrology and Kidney Transplant Wards of a Referral Academic Hospital. *J Res Pharm Pract* **2016,** *5* (1), 43-51.
4. *Report on the Burden of Endemic Health Care-Associated Infection Worldwide*. World Health Organization (WHO): 2011.
5. Collins, A., Preventing Health Care–Associated Infections. In *Patient Safety and Quality: An Evidence-Based Handbook for Nurses.*, Agency for Healthcare Research and Quality (US): April 2008.
6. Wainwright, M.; Phoenix, D. A.; Marland, J.; Wareing, D. R. A.; Bolton, F. J., A Study of Photobactericidal Activity in the Phenothiazinium Series. *FEMS Immunol. Med. Microbiol.* **1997,** *19* (1), 75-80.
7. Wainwright, M.; Crossley, K. B., Photosensitising Agents - Circumventing Resistance and Breaking Down Biofilms: A Review. *Int. Biodeterior. Biodegrad.* **2004,** *53* (2), 119-126.
8. Demidova, T. N.; Hamblin, M. R., Photodynamic Inactivation of Bacillus Spores, Mediated by Phenothiazinium Dyes. *Appl. Environ. Microbiol.* **2005,** *71* (11), 6918-6925.
9. Meisel, P.; Kocher, T., Photodynamic Therapy for Periodontal Diseases: State of the Art. *J. Photochem. Photobiol. B-Biol.* **2005,** *79* (2), 159-170.
10. Saji, M.; Taguchi, S.; Uchiyama, K.; Osono, E.; Hayama, N.; Ohkuni, H., Efficacy of Gentian-Violet in the Eradication of Methicillin-Resistant Staphylococcus-Aureus from Skin-Lesions. *J Hosp Infect* **1995,** *31* (3), 225-228.
11. Perni, S.; Piccirillo, C.; Pratten, J.; Prokopovich, P.; Chrzanowski, W.; Parkin, I. P.; Wilson, M., The Antimicrobial Properties of Light-Activated Polymers Containing Methylene Blue and Gold Nanoparticles. *Biomaterials* **2009,** *30* (1), 89-93.
12. Perni, S.; Prokopovich, P.; Piccirillo, C.; Pratten, J.; Parkin, I. P.; Wilson, M., Toluidine Blue-Containing Polymers Exhibit Potent Bactericidal Activity when Irradiated with Red Laser Light. *J Mater Chem* **2009,** *19* (18), 2715-2723.
13. Noimark, S.; Dunnill, C. W.; Kay, C. W. M.; Perni, S.; Prokopovich, P.; Ismail, S.; Wilson, M.; Parkin, I. P., Incorporation of Methylene Blue and Nanogold into Polyvinyl Chloride Catheters; A New Approach for Light-Activated Disinfection of Surfaces. *J Mater Chem* **2012,** *22* (30), 15388-15396.

14. Noimark, S.; Bovis, M.; MacRobert, A. J.; Correia, A.; Allan, E.; Wilson, M.; Parkin, I. P., Photobactericidal Polymers; The Incorporation of Crystal Violet and Nanogold into Medical Grade Silicone. *RSC Adv* **2013,** *3* (40), 18383-18394.
15. Dolmans, D. E.; Fukumura, D.; Jain, R. K., Photodynamic Therapy for Cancer. *Nat Rev Cancer* **2003,** *3* (5), 380-387.
16. Alivisatos, A. P.; Gu, W. W.; Larabell, C., Quantum Dots as Cellular Probes. *Annu. Rev. Biomed. Eng.* **2005,** *7*, 55-76.
17. Samia, A. C. S.; Dayal, S.; Burda, C., Quantum Dot-Based Energy Transfer: Perspectives and Potential for Applications in Photodynamic Therapy. *Photochem Photobiol* **2006,** *82* (3), 617-625.
18. Gill, R.; Zayats, M.; Willner, I., Semiconductor Quantum Dots for Bioanalysis. *Angew. Chem., Int. Ed. Eng.* **2008,** *47* (40), 7602-7625.
19. Yu, W. W.; Chang, E.; Drezek, R.; Colvin, V. L., Water-Soluble Quantum Dots for Biomedical Applications. *Biochem. Biophys. Res. Commun.* **2006,** *348* (3), 781-786.
20. Resch-Genger, U.; Grabolle, M.; Cavaliere-Jaricot, S.; Nitschke, R.; Nann, T., Quantum Dots versus Organic Dyes as Fluorescent Labels. *Nat Methods* **2008,** *5* (9), 763-775.
21. Xu, G. X.; Zeng, S. W.; Zhang, B. T.; Swihart, M. T.; Yong, K. T.; Prasad, P. N., New Generation Cadmium-Free Quantum Dots for Biophotonics and Nanomedicine. *Chem Rev* **2016,** *116* (19), 12234-12327.
22. Yaghini, E.; Seifalian, A. M.; MacRobert, A. J., Quantum Dots and their Potential Biomedical Applications in Photosensitization for Photodynamic Therapy. *Nanomedicine (Lond.)* **2009,** *4* (3), 353-363.
23. Courtney, C. M.; Goodman, S. M.; McDaniel, J. A.; Madinger, N. E.; Chatterjee, A.; Nagpal, P., Photoexcited Quantum Dots for Killing Multidrug-Resistant Bacteria. *Nat Mater* **2016,** *15* (5), 529-534.
24. Ipe, B. I.; Lehnig, M.; Niemeyer, C. M., On the Generation of Free Radical Species from Quantum Dots. *Small* **2005,** *1* (7), 706-709.
25. Narband, N.; Mubarak, M.; Ready, D.; Parkin, I. P.; Nair, S. P.; Green, M. A.; Beeby, A.; Wilson, M., Quantum Dots as Enhancers of the Efficacy of Bacterial Lethal Photosensitization. *Nanotechnology* **2008,** *19* (44).
26. Ristic, B. Z.; Milenkovic, M. M.; Dakic, I. R.; Todorovic-Markovic, B. M.; Milosavljevic, M. S.; Budimir, M. D.; Paunovic, V. G.; Dramicanin, M. D.; Markovic, Z. M.; Trajkovic, V. S., Photodynamic Antibacterial Effect of Graphene Quantum Dots. *Biomaterials* **2014,** *35* (15), 4428-4435.
27. Chibli, H.; Carlini, L.; Park, S.; Dimitrijevic, N. M.; Nadeau, J. L., Cytotoxicity of InP/ZnS Quantum Dots Related to Reactive Oxygen Species Generation. *Nanoscale* **2011,** *3* (6), 2552-2559.
28. Ge, J.; Lan, M.; Zhou, B.; Liu, W.; Guo, L.; Wang, H.; Jia, Q.; Niu, G.; Huang, X.; Zhou, H.; Meng, X.; Wang, P.; Lee, C. S.; Zhang, W.; Han, X., A Graphene Quantum Dot Photodynamic Therapy Agent with High Singlet Oxygen Generation. *Nat Commun* **2014,** *5*, 4596.
29. Ge, J. C.; Lan, M. H.; Liu, W. M.; Jia, Q. Y.; Guo, L.; Zhou, B. J.; Meng, X. M.; Niu, G. L.; Wang, P. F., Graphene Quantum Dots as Efficient, Metal-Free, Visible-Light-Active Photocatalysts. *Sci China Mater* **2016,** *59* (1), 12-19.
30. Yaghini, E.; Pirker, K. F.; Kay, C. W. M.; Seifalian, A. M.; MacRobert, A. J., Quantification of Reactive Oxygen Species Generation by Photoexcitation of PEGylated Quantum Dots. *Small* **2014,** *10* (24), 5106-5115.
31. Moeno, S.; Antunes, E.; Khene, S.; Litwinski, C.; Nyokong, T., The Effect of Substituents on the Photoinduced Energy Transfer between CdTe Quantum Dots and Mercapto Substituted Zinc Phthalocyanine Derivatives. *Dalton T* **2010,** *39* (14), 3460-3471.
32. Charron, G.; Stuchinskaya, T.; Edwards, D. R.; Russell, D. A.; Nann, T., Insights into the Mechanism of Quantum Dot-Sensitized Singlet Oxygen Production for Photodynamic Therapy. *J Phys Chem C* **2012,** *116* (16), 9334-9342.
33. Derfus, A. M.; Chan, W. C. W.; Bhatia, S. N., Probing the Cytotoxicity of Semiconductor Quantum Dots. *Nano Lett* **2004,** *4* (1), 11-18.
34. Cho, S. J.; Maysinger, D.; Jain, M.; Roder, B.; Hackbarth, S.; Winnik, F. M., Long-Term Exposure to CdTe Quantum Dots Causes Functional Impairments in Live Cells. *Langmuir* **2007,** *23* (4), 1974-1980.
35. Yaghini, E.; Turner, H. D.; Le Marois, A. M.; Suhling, K.; Naasani, I.; MacRobert, A. J., In vivo biodistribution studies and ex vivo lymph node imaging using heavy metal-free quantum dots. *Biomaterials* **2016,** *104*, 182-191.
36. Yaghini, E.; Turner, H.; Pilling, A.; Naasani, I.; MacRobert, A. J., In Vivo Biodistribution and Toxicology Studies of Cadmium-Free Indium-Based Quantum Dot Nanoparticles in a Rat Model. *Nanomedicine (Lond.)* **2018,** *14* (8), 2644-2655.

37. Pikett N, D. S., Mushtaq I Preparation of Nanoparticle Materials. US 7,588,828 B2, Sep 15, 2009.
38. Sehmi, S. K.; Noimark, S.; Bear, J. C.; Peveler, W. J.; Bovis, M.; Allan, E.; MacRobert, A. J.; Parkin, I. P., Lethal Photosensitisation of Staphylococcus aureus and Escherichia coli Using Crystal Violet and Zinc Oxide-Encapsulated Polyurethane. *J Mater Chem B* **2015,** *3* (31), 6490-6500.
39. Maley, A. M.; Arbiser, J. L., Gentian Violet: A 19th Century Drug Re-Emerges in the 21st Century. *Exp Dermatol* **2013,** *22* (12), 775-780.
40. Arbiser, J. L., Gentian Violet is Safe. *J Am Acad Dermatol* **2009,** *61* (2), 359-359.
41. Berrios, R. L.; Arbiser, J. L., Effectiveness of Gentian Violet and Similar Products Commonly Used to Treat Pyodermas. *Dermatol Clin* **2011,** *29* (1), 69-73.
42. Dimitrijevic, N. M.; Takahashi, K.; Jonah, C. D., Visible Absorption Spectra of Crystal Violet in Supercritical Ethane-Methanol Solution. *J Supercrit Fluid* **2002,** *24* (2), 153-159.
43. Oliveira, C. S.; Branco, K. P.; Baptista, M. S.; Indig, G. L., Solvent and Concentration Effects on the Visible Spectra of Tri-Para-Dialkylamino-Substituted Triarylmethane Dyes in Liquid Solutions. *Spectroc. Acta Pt. A-Molec. Biomolec. Spectr.* **2002,** *58* (13), 2971-2982.
44. Brey, L. A.; Schuster, G. B.; Drickamer, H. G., High-Pressure Studies of Effect of Viscosity on Fluorescence Efficiency in Crystal Violet and Auramine O. *J Chem Phys* **1977,** *67* (6), 2648-2650.
45. Cremers, D. A.; Windsor, M. W., A Study of the Viscosity-Dependent Electronic Relaxation of Some Triphenylmethane Dyes Using Picosecond Flash-Photolysis. *Chemical Physics Letters* **1980,** *71* (1), 27-32.
46. Baptista, M. S.; Indig, G. L., Effect of BSA Binding on Photophysical and Photochemical Properties of Triarylmethane Dyes. *J Phys Chem B* **1998,** *102* (23), 4678-4688.
47. *Global Priority List of Antibiotic-Resistant Bacteria to Guide Research, Discovery and Development of New Antibiotics*; World Health Organization (WHO): 2017.
48. Silhavy, T. J.; Kahne, D.; Walker, S., The Bacterial Cell Envelope. *Cold Spring Harb Perspect Biol* **2010,** *2* (5), a000414.
49. Crick, C. R.; Noimark, S.; Peveler, W. J.; Bear, J. C.; Ivanov, A. P.; Edel, J. B.; Parkin, I. P., Advanced Analysis of Nanoparticle Composites - A Means toward Increasing the Efficiency of Functional Materials. *RSC Adv* **2015,** *5* (66), 53789-53795.
50. Devatha, G.; Roy, S.; Rao, A.; Mallick, A.; Basu, S.; Pillai, P. P., Electrostatically Driven Resonance Energy Transfer in "Cationic" Biocompatible Indium Phosphide Quantum Dots. *Chem Sci* **2017,** *8* (5), 3879-3884.
51. Issac, A.; Jin, S. Y.; Lian, T. Q., Intermittent Electron Transfer Activity from Single CdSe/ZnS Quantum Dots. *J. Am. Chem. Soc.* **2008,** *130* (34), 11280-11281.
52. Lakowicz, J. R., *Principles of Fluorescence Spectroscopy*. 3rd ed. ed.; New York : Springer: New York, 2006.
53. Medintz, I. L.; Mattoussi, H., Quantum Dot-Based Resonance Energy Transfer and its Growing Application in Biology. *Phys Chem Chem Phys* **2009,** *11* (1), 17-45.
54. Murphy, C. B.; Zhang, Y.; Troxler, T.; Ferry, V.; Martin, J. J.; Jones, W. E., Probing Forster and Dexter Energy-Transfer Mechanisms in Fluorescent Conjugated Polymer Chemosensors. *J Phys Chem B* **2004,** *108* (5), 1537-1543.
55. Naguib, Y. M. A.; Steel, C.; Cohen, S. G.; Young, M. A., Triplet-Sensitized Photobleaching of Crystal Violet. *J. Photochem. Photobiol. A-Chem.* **1996,** *96* (1-3), 149-154.
56. Huston, A. L.; Justus, B. L.; Campillo, A. J., Direct Measurement of the Viscosity of Glycerol under Laser Driven Shock Compression - Fluorescence Lifetime Changes in Crystal Violet. *Chem. Phys. Lett.* **1985,** *122* (6), 617-621.
57. Sillen, A.; Engelborghs, Y., The Correct Use of "Average" Fluorescence Parameters. *Photochem Photobiol* **1998,** *67* (5), 475-486.
58. Sadhu, S.; Haldar, K. K.; Patra, A., Size Dependent Resonance Energy Transfer between Semiconductor Quantum Dots and Dye using FRET and Kinetic Model. *J Phys Chem C* **2010,** *114* (9), 3891-3897.
59. Noimark, S.; Salvadori, E.; Gomez-Bombarelli, R.; MacRobert, A. J.; Parkin, I. P.; Kay, C. W. M., Comparative Study of Singlet Oxygen Production by Photosensitiser Dyes Encapsulated in Silicone: Towards Rational Design of Anti-Microbial Surfaces. *Phys Chem Chem Phys* **2016,** *18* (40), 28101-28109.
60. Yaghini, E.; Giuntini, F.; Eggleston, I. M.; Suhling, K.; Seifalian, A. M.; MacRobert, A. J., Fluorescence Lifetime Imaging and FRET-Induced Intracellular Redistribution of Tat-Conjugated Quantum Dot Nanoparticles through Interaction with a Phthalocyanine Photosensitiser. *Small* **2014,** *10* (4), 782-792.

61. Bovis, M. J.; Noimark, S.; Woodhams, J. H.; Kay, C. W. M.; Weiner, J.; Peveler, W. J.; Correia, A.; Wilson, M.; Allan, E.; Parkin, I. P.; MacRobert, A. J., Photosensitisation Studies of Silicone Polymer Doped with Methylene Blue and Nanogold for Antimicrobial Applications. *RSC Adv* **2015,** *5* (68), 54830-54842.
62. Armstrong, D. A.; Huie, R. E.; Koppenol, W. H.; Lymar, S. V.; Merenyi, G.; Neta, P.; Ruscic, B.; Stanbury, D. M.; Steenken, S.; Wardman, P., Standard Electrode Potentials Involving Radicals in Aqueous Solution: Inorganic Radicals (IUPAC Technical Report). *Pure Appl. Chem.* **2015,** *87* (11-12), 1139-1150.
63. Rao, P. S.; Hayon, E., Reduction of Dyes by Free-Radicals in Solution - Correlation between Reaction-Rate Constants and Redox Potentials. *J. Phys. Chem.* **1973,** *77* (23), 2753-2756.
64. Blackburn, J. L.; Selmarten, D. C.; Ellingson, R. J.; Jones, M.; Micic, O.; Nozik, A. J., Electron and Hole Transfer from Indium Phosphide Quantum Dots. *J Phys Chem B* **2005,** *109* (7), 2625-2631.
65. Reszka, K.; Cruz, F. S.; Docampo, R., Photosensitization by the Trypanocidal Agent Crystal Violet - Type-I versus Type-II Reactions. *Chem.-Biol. Interact.* **1986,** *58* (2), 161-172.
66. Fischer, V.; Harrelson, W. G.; Chignell, C. F.; Mason, R. P., Spectroscopic Studies of Cutaneous Photosensitizing Agents 5. Spin Trapping and Direct Electron-Spin Resonance Investigations of the Photoreduction of Gentian (Crystal) Violet. *Photobioch Photobiop* **1984,** *7* (2), 111-119.
67. Oliveira, C. S.; Turchiello, R.; Kowaltowski, A. J.; Indig, G. L.; Baptista, M. S., Major Determinants of Photoinduced Cell Death: Subcellular Localization versus Photosensitization Efficiency. *Free Radic. Biol. Med.* **2011,** *51* (4), 824-833.
68. Brezova, V.; Pigosova, J.; Havlinova, B.; Dvoranova, D.; Durovic, M., EPR Study of Photochemical Transformations of Triarylmethane Dyes. *Dyes Pigment.* **2004,** *61* (2), 177-198.
69. Bacellar, I. O. L.; Oliyeira, M. C.; Dantas, L. S.; Costa, E. B.; Junqueira, H. C.; Martins, W. K.; Durantini, A. M.; Cosa, G.; Di Mascio, P.; Wainwright, M.; Miotto, R.; Cordeiro, R. M.; Miyamoto, S.; Baptista, M. S., Photosensitized Membrane Permeabilization Requires Contact-Dependent Reactions between Photosensitizer and Lipids. *J. Am. Chem. Soc.* **2018,** *140* (30), 9606-9615.

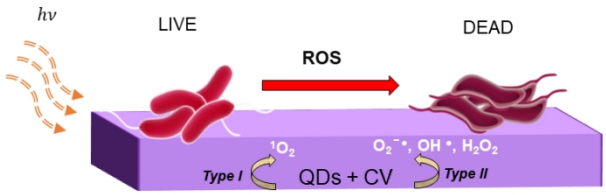

338x190mm (96 x 96 DPI)